Neutron scattering study of spin fluctuations in $Y(Mn_{1-x}Al_x)_2$

K. Motoya
Department of Physics, Faculty of Science, Saitama University, 255 Shimo-Okubo, Urawa, Saitama 338, Japan

T. Freltoft, P. Böni, and G. Shirane
Department of Physics, Brookhaven National Laboratory, Upton, New York 11973-5000
(Received 8 April 1988)

Elastic and inelastic neutron-scattering measurements have been made on a series of pseudobinary intermetallic compounds $Y(Mn_{1-x}Al_x)_2$. Long-range antiferromagnetic order below $T_N \sim 100$ K in YMn_2 has been shown to collapse by substitution of only 5% of the manganese atoms by aluminum atoms. In these compounds, a spin-glass transition has been clearly indicated by a change in the energy width of the scattered-neutron spectrum, as well as by the onset of field hysteresis in susceptibility measurements. In the compound with $x=0.10$, the amplitude of spin fluctuations S does not change appreciably with temperature, whereas in YMn_2 it drops by more than 30% at T_N and then increases gradually with increasing temperature. A considerable degree of spatial correlations of spin fluctuations persists up to at least 760 K, which is similar to the behavior observed in YMn_2 but quite different from the characteristics of simple localized-electron magnets.

I. INTRODUCTION

The study of metallic magnetism has a long history in which the theory of spin fluctuations has been a leading factor towards a unified understanding of the magnetism in a wide variety of metallic materials.[1,2] In this theory all the magnetic properties are directly deduced from the nature of spin fluctuations, i.e., localization and amplitude of the magnetic moment.

Theoretically, much effort has been concentrated to establish a general method which reproduces the spatial and temporal behavior of the spin fluctuations and therefore the magnetic properties of a particular material, deduced from a small number of its characteristic physical parameters. The self-consistent renormalization theory of spin fluctuations has been successful in describing physical properties of a group of materials classified as weak ferromagnets or antiferromagnets. In these materials, the local amplitude of the spin fluctuations is small at low temperatures and increases with increasing temperature. The spin fluctuation components around the origin (or antiferromagnetic vector) are enhanced, which means that the spin fluctuations are extended in real space. The opposite limiting case, the local moment limit, has also a well-founded theory where the local amplitude of the spin density is temperature independent and the spin fluctuations are localized in real space.

Most of the metallic magnetic materials are, according to their characteristics of the spin fluctuations, scattered between the two limiting cases mentioned above. However, no universal theory dealing with their magnetic properties has yet been established. Much effort is currently made to develop a unified theory applicable to the intermediate range.[2]

Experimentally, several aspects of spin fluctuations in many different materials have been extensively studied using various methods. Among these aspects the behavior of spin fluctuations above the transition temperature is very important since the different characteristics are much more pronounced above T_c (or T_N). However, the most important information, namely the spatial correlations and the local amplitude of the spin fluctuations, can only be directly obtained using neutron-scattering techniques. Recently the technique has been applied to several metallic magnets.[3] These materials include the Heusler alloy Pd_2MnSn (which has been regarded as a typical example of a local-moment system), MnSi (a weakly itinerant electron ferromagnet), and materials located between them (such as Fe, Ni, and Fe_3Pt). The spin fluctuation behavior observed in the two limiting materials are quite different from each other. In Pd_2MnSn the overall static and dynamical response of neutrons can be basically interpreted based on Heisenberg-type interactions between localized spins, although it has been recently detected[4] that nonadiabatic effects for the conduction electrons at high temperatures are also important. On the other hand, in MnSi (Ref. 5) the scattering intensity strongly depends on wave vector even at $T \sim 10T_c$. These observations for MnSi agree remarkably well with the prediction from the self-consistent renormalization theory.

For the intermediate case experimental information is rather limited concerning the number of materials investigated. Moreover, covered temperature and energy ranges are often insufficient to characterize their spin fluctuation properties completely. In order to stimulate theoretical development, detailed neutron scattering experiments of many materials covering a whole region between local moment magnetism and weakly itinerant electron magnetism are highly needed. The present work, we believe, contributes to the above-mentioned course of study.

The cubic Laves-phase intermetallic compound YMn_2 was regarded as a Pauli paramagnet. Recent neutron-diffraction experiments, however, revealed that it orders antiferromagnetically below $T_N \sim 100$ K.[6,7] The amplitude of the magnetic moment in the antiferromagnetic phase determined in Ref. 6 is $2.7\mu_B$ / Mn-atom. However, susceptibility[8] and NMR relaxation behavior[9] in the paramagnetic phase are similar to those of weakly itinerant electron magnets and are incompatible with the large local moments observed in the ordered phase. Moreover, a significant volume change of $\sim 6\%$ at $T = T_N$ with a large thermal hysteresis[8] strongly suggests that the local magnetic moments collapse at $T = T_N$.

Magnetic properties of pseudobinary compounds $Y(Mn_{1-x}Al_x)_2$ were also studied by means of susceptibility, thermal expansion, and NMR experiments.[10,11] The sharp volume change observed in YMn_2 at $T = T_N$ becomes less pronounced and the susceptibility behavior becomes more temperature dependent as the Al concentration increases. For compounds with $x \geq 0.1$, the sharp volume change disappears and a Curie-Weis–type susceptibility develops at higher temperatures with a pronounced maximum at low temperatures.

These observations suggest that a transition from predominantly local-moment magnetism in the low-temperature phase to weakly itinerant electron magnetism in the high-temperature phase takes place at $T = T_N$ in YMn_2 and that a similar transition also takes place in $Y(Mn_{1-x}Al_x)_2$ as the concentration x is increased. If these conjectures are true, we can expect to derive useful information from microscopic studies on this material leading us towards a unified understanding of metallic magnetism. This idea prompted us to perform a neutron scattering study on a series of intermetallic compounds $Y(Mn_{1-x}Al_x)_2$.

Results of paramagnetic neutron scattering experiments on YMn_2 has already been reported by Deportes *et al.*[12,13] and the present authors.[14,15] Neutron diffraction and susceptibility measurements of $Y(Mn_{1-x}Al_x)_2$ mainly concerning with spin glass behavior at low temperatures have also been reported by one of the present authors,[16] and energy integrated paramagnetic neutron-scattering measurements on $Y(Mn_{0.9}Al_{0.1})_2$ up to $T = 300$ K were also published in Ref. 13.

In this paper we report mainly on neutron scattering results of $Y(Mn_{0.9}Al_{0.1})_2$ with contrast to those of YMn_2. Sample characteristics and experimental details are described in Sec. II. Results are reported in Sec. III, and in Sec. IV a discussion of the results is presented.

II. EXPERIMENTAL DETAILS

A. Sample

Intermetallic compounds of $Y(Mn_{1-x}Al_x)_2$ with $x = 0$, 0.05, 0.10, and 0.20 were prepared by argon arc melting. The purity of the component metals is 99.9% and the atomic ratio of the starting materials was chosen to have [Y]/[(Mn,Al)] = 1.05/2.00. The excess amount of Y metal was added to avoid possible formation of Mn-rich ferromagnetic compounds such as Y_6Mn_{23}. The ingot was annealed at 800 °C for a week then crushed into powder. Powder x-ray diffraction patterns show traces of Y metal, but the existence of any metallic compound structures besides the Cu_2Mg structure was not detected.

Magnetic susceptibility of the pseudobinary compounds were measured utilizing a variable-temperature SQUID (superconducting quantum interference device) magnetometer in the temperature range 6–300 K. Spin glass transitions were indicated by field cooled effects below $T_{SG} \sim 60$, 50, and 40 K for compounds with $x = 0.05$, 0.10, and 0.20, respectively.[16]

B. Neutron scattering

Polarized neutron scattering measurements[17,18] were performed on a triple axis spectrometer at the High Flux Beam Reactor of Brookhaven National Laboratory. The polarization direction **P** of the incident neutrons was selected by a Heusler crystal. A weak magnetic field (~ 20 Oe) was applied at the sample position to guide the neutron polarization either parallel (horizontal field, HF) or perpendicular (vertical field, VF) to the scattering vector **Q**. The polarization direction of the scattered neutrons was reversed by a flat coil spin flipper placed before a Heusler analyzer which selects neutron energy and polarization. Various combinations of the fixed final neutron energy and the horizontal beam collimation were utilized according to the kind of measurements. The overall instrumental flipping ratio was better than $R \sim 15$ throughout the experiment. A pair of scattering intensities, spin-flip intensity with $\mathbf{P} \| \mathbf{Q}$ [$I^{+-}(\mathbf{P} \| \mathbf{Q})$] and spin-flip intensity with $\mathbf{P} \perp \mathbf{Q}$ [$I^{+-}(\mathbf{P} \perp \mathbf{Q})$] were collected. The difference between these intensities, $(I_{HF} - I_{VF})$ which is free from various background scattering contributions, corresponds to one-half of the magnetic scattering intensity measured in unpolarized beam experiments. These measurements were performed for the momentum transfer range of $0.5 \leq Q \leq 2.5$ Å^{-1} and temperature range of 5–766 K.

In order to check the overall performance of the present experimental setup and also to confirm the accuracy of the analysis procedure, we measured paramagnetic scattering intensities from powdered MnF_2, which is a typical local-moment antiferromagnet. The moment value determined through the same procedure as was taken for the present compound system agrees with what is expected for $S = \frac{5}{2}$ of the Mn^{2+} ion within 10% over the temperature range 75.7–207 K ($1.13 \leq T/T_N \leq 3.08$).

III. RESULTS AND ANALYSIS

In Fig. 1 we show inelastic neutron scattering spectra of $Y(Mn_{0.9}Al_{0.1})_2$ for momentum transfer $Q = 1.80$ Å^{-1} at various temperatures. The measurements were made with spin-flipper ON (spin-flip scattering) and the intensity $I_{HF} - I_{VF}$ means the difference between $I^{+-}(\mathbf{P} \| \mathbf{Q})$ and $I^{+-}(\mathbf{P} \perp \mathbf{Q})$ as explained in Sec. II. Correction for the misalignment of the horizontal field direction with the scattering vector encountered at points for $E \neq 0$ has already been applied. Instrumental parameters for each

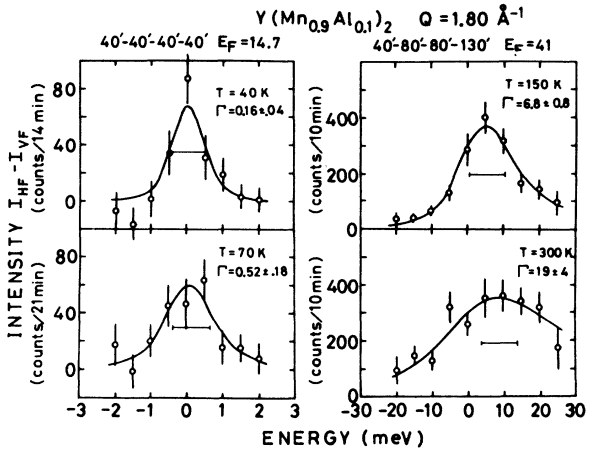

FIG. 1. Neutron scattering spectra obtained using the parallel-perpendicular method (I_{HF}-I_{VF}) of $Y(Mn_{0.9}Al_{0.1})_2$ at various temperatures. Measurements were made with a momentum transfer $Q=1.80$ Å^{-1}. The curves are fit of Lorentzian line shapes to the data including various corrections described in the text. Instrumental resolutions ($2\Gamma_{res}$) for each experimental condition are shown by horizontal bars.

group of measurements are posted above the frames. The energy width of scattered neutrons increases rapidly with temperature. Above 300 K, the complete spectrum cannot be covered with the present experimental conditions.

The cross section for magnetic neutron scattering is expressed by

$$\frac{d^2\sigma}{d\omega\, d\Omega}=\gamma_0^2 f^2(\mathbf{Q})e^{-2W}S(\mathbf{q},\omega)\ , \tag{1}$$

where γ_0^2, $f(\mathbf{Q})$, e^{-2W} are 0.291 barn, the magnetic form factor as a function of scattering vector $\mathbf{Q}$ measured with respect to direct beam, and the Debye-Waller factor, respectively. The symbol $\mathbf{q}$ means the wave vector relative to the nearest magnetic reciprocal lattice point. For relatively small $\mathbf{q}$ and ω, the scattering function can be expressed as

$$S(\mathbf{q},\omega)=M^2(\mathbf{q})\frac{1}{\pi}\frac{\Gamma_q}{\Gamma_q^2+\omega^2}\frac{\hbar\omega/k_BT}{1-e^{-\hbar\omega/k_BT}} \tag{2}$$

in which

$$M^2(\mathbf{q})=M^2(0)\frac{\kappa_1^2}{\kappa_1^2+q^2}\ , \tag{3}$$

where Γ_q and κ_1 are the energy line width and the inverse correlation length, respectively. For a Heisenberg antiferromagnet Γ_q varies with q as

$$\Gamma_q\sim q^{1.5} \tag{4}$$

for small q,[19] but does not strongly depend on temperature,[20] whereas in weakly itinerant electron antiferromagnets Γ_Q varies as[2]

$$\Gamma_Q=\Gamma_{G+q}\sim(q^2+\kappa_G^2)\ , \tag{5}$$

where $\mathbf{G}$ is the antiferromagnetic vector and the parameter κ_G varies with T.

In the present powder sample experiment, the observed intensity is composed of scattering from an enormous number of randomly oriented crystallites. In a constant-$\mathbf{Q}$ measurement, the momentum transfer $\mathbf{q}$ measured from a magnetic Bragg point is different for each crystallite depending on the orientation of its crystal axis. Therefore, the energy spectrum pattern may not necessarily be a simple Lorentzian as for the case of single-crystal experiments. However, the observed pattern is practically traced by a Lorentzian curve probably due to the combined effect of the powder average and limited energy resolution. The curves in Fig. 1 show the results of least-square fit to a Lorentzian line shape including instrumental energy resolution and thermal factor. The obtained Γ values are shown in the figure.

We show in Fig. 2 the temperature variation of the energy width Γ for $Y(Mn_{0.9}Al_{0.1})_2$ measured at $Q=1.8$ Å^{-1}. At low temperatures, the energy width is indistinguishable from the instrumental resolution. Above $T_{SG}\sim 50$ K, Γ increases almost linearly with temperature and it tends to saturate above $\Gamma\sim 300$ K. The meaning of the curve will be described in Sec. IV.

As we mentioned above, the energy spectra of scattered neutrons are reasonably well fitted by Lorentzian functions within the measured spectrum range, so we integrated the fitted Lorentzian over the entire range beyond the ends of the data points. This integration is considered to give an upper limit of the integrated intensity and therefore of the cross section as discussed later. The energy scan and the integration was conducted for only some selected Q points. For other Q points, the energy integrated intensities were estimated from the intensities at $E=0$ assuming an appropriate spectral width. These integrated intensities were then converted to absolute cross sections per Mn atom by comparing with the intensity of a nuclear Bragg peak measured at the same temperature.

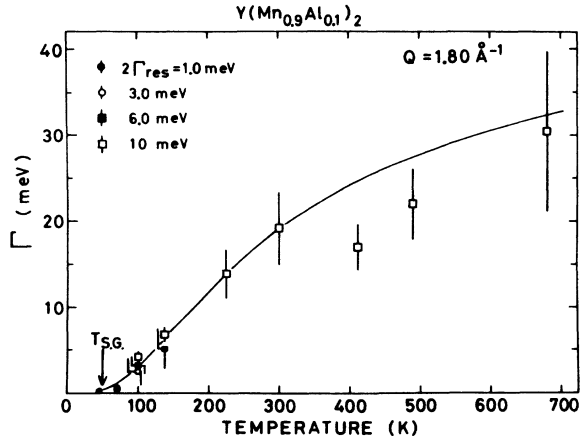

FIG. 2. Temperature variation of the energy width of scattered neutrons from $Y(Mn_{0.9}Al_{0.1})_2$ at $Q=1.80$ Å^{-1}. The meaning of the curve is described in the text.

Figure 3 shows energy integrated magnetic scattering cross sections as a function of momentum transfer of YMn_2 (b) and $Y(Mn_{0.9}Al_{0.1})_2$ (c) at representative temperatures. The polarized neutron-diffraction pattern of YMn_2 in the antiferromagnetic phase at 10 K is also shown for comparison (a). The solid circles at $Q=0$ represent calculated neutron cross sections from static susceptibility measurements, where the data for YMn_2 were taken from Ref. 10.

In $Y(Mn_{0.9}Al_{0.1})_2$ no magnetic Bragg peaks exist even at the lowest temperature. Instead, diffuse scattering patterns similar to those seen in YMn_2 above T_N are observed throughout the covered temperature range. The width of the diffuse peaks becomes broader when the temperature is increased, however, even at the highest temperature $T=766$ K the scattering pattern is still different from that observed in local-moment systems far above the ordering temperature, where the magnetic scattering is entirely incoherent and the cross section decreases monotonically with increasing Q due to the magnetic form factor [see the broken line in Fig. 3(b)]. The observed Q-dependent scattering indicates that the magnetic correlations persist in the high-temperature phase of $Y(Mn_{0.9}Al_{0.1})_2$ as was the case in YMn_2. Moreover, the fact that the observed peak position nearly corresponds to that of the most intense magnetic Bragg peak in the antiferromagnetic phase of YMn_2, indicates that the magnetic correlations in $Y(Mn_{0.9}Al_{0.1})_2$ are also based on the antiferromagnetic structure of YMn_2.

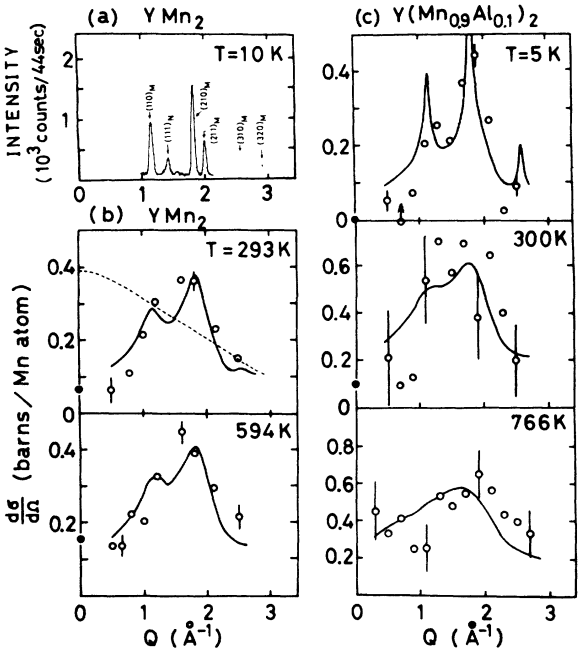

FIG. 3. (a) Neutron-diffraction pattern of YMn_2 at $T=10$ K. Magnetic peaks are enhanced by polarization analysis. Dashed lines are the results of the unpolarized neutron experiment. (b) and (c) Energy integrated cross sections as a function of momentum transfer of YMn_2 and $Y(Mn_{0.9}Al_{0.1})_2$. The absolute scale is obtained by normalizing to a nuclear Bragg peak. Points shown for $Q=0$ are calculated from static susceptibility data. (Data for YMn_2 are taken from Ref. 9). Solid curves show model calculations best fitted to the data described in the text. The dashed curve corresponds to the cross section for an ideal paramagnet with spin $S=1$.

Patterns shown in Figs. 3(b) and 3(c) are the results of powder averages of the cross section given by Eq. (1), i.e., the intensity contribution to a specific Q consists of the sum of $S(\mathbf{q},\omega)$ in which $\mathbf{q}$ satisfies $|\mathbf{Q}|=|\mathbf{G}+\mathbf{q}|$, where $\mathbf{G}$ represents the wave vector for the nearest magnetic Bragg peaks. We divide the reciprocal space of each crystallite into intensity zones (IZ) centered around each magnetic Bragg point. The extent of an IZ is defined so that a general point in $\mathbf{Q}$ space belongs to the IZ centered around the nearest magnetic Bragg point. At the center of each IZ, the function of Eq. (3) has its maximum and it extends to the IZ boundary. The relative amplitude of the peak is scaled according to the static magnetic structure factor. The observed scattering pattern is the sum of contributions from randomly oriented crystallites. We obtained parameters $M(0)$and κ_1 by a least-square fitting procedure. Due to the powder smearing, $M(0)$ and κ_1 are very strongly correlated. Hence, the absolute value of each of the parameters is determined by only $\pm 50\%$. The result of the fitting is represented by the curves in Figs. 3(b) and 3(c).

Temperature variations of the inverse correlation length κ_1 of YMn_2 and $Y(Mn_{0.9}Al_{0.1})_2$ are shown in Fig. 4. The result for MnF_2, which is known to be a typical local-moment antiferromagnet is also shown in the figure. In MnF_2, κ_1 increases rapidly demonstrating that the magnetic correlations quickly disappear above T_N as expected for a local-moment Heisenberg system. The behavior for YMn_2 and $(Mn_{0.9}Al_{0.1})_2$ is quite different from that of MnF_2. In YMn_2, the inverse correlation length jumps to the small finite value at T_N. However, it does not increase appreciably up to above $\sim 6T_N$. The behav-

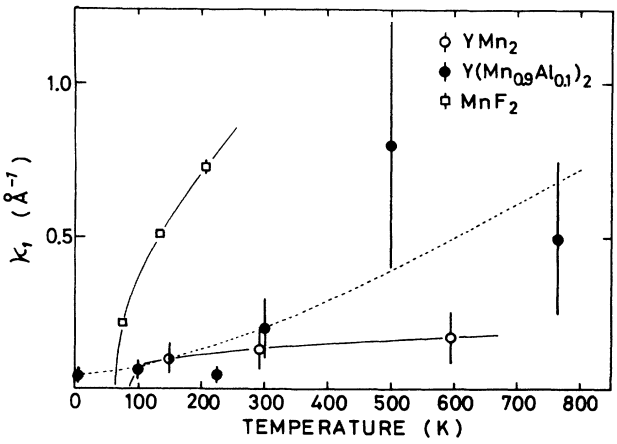

FIG. 4. Temperature variations of inverse correlation length obtained from the fits shown in Fig. 3 for YMn_2, $Y(Mn_{0.9}Al_{0.1})_2$, and MnF_2. Curves are drawn to guide the eye.

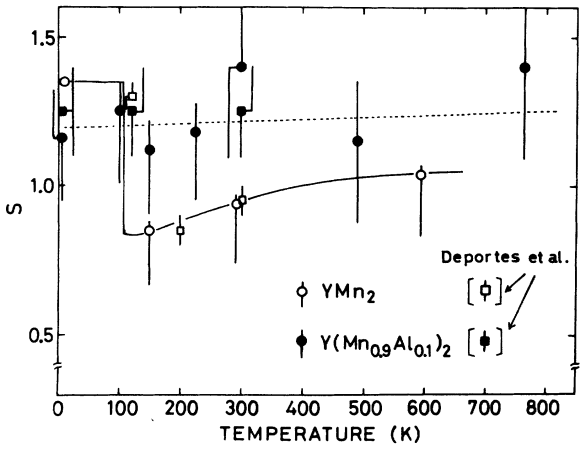

FIG. 5. Temperature variations of the local amplitude of spin fluctuations per Mn atom for YMn_2 and $Y(Mn_{0.9}Al_{0.1})_2$. Values after Deportes *et al.* (Ref. 13) are also included in the figure. Curves are drawn to guide the eye.

ior for $Y(Mn_{0.9}Al_{0.1})_2$ is something between the two above cases.

The amplitude of local spin density fluctuations S, hereafter denoted as the spin, is then calculated from $M^2(\mathbf{q})$ by averaging over the IZ as

$$4S(S+1)=\frac{1}{V_{\mathrm{IZ}}}\int_{\mathrm{IZ}} M^2(\mathbf{q})d^3q \ . \tag{6}$$

The integration over the IZ was substituted by the integration over a sphere with the same volume as the actual IZ. We note that even though the absolute values of $M^2(0)$ and κ_1 are not very well determined, the IZ average as represented by Eq. (6) is very insensitive to the combined set of the two parameters.

Temperature variations of the spin S per Mn atom for YMn_2 and $Y(Mn_{0.9}Al_{0.1})_2$ obtained from the above mentioned procedure are shown in Fig. 5. In this figure solid and open circles show the values corresponding to the energy integrations over the full Lorentzian width of the scattered energy spectra and therefore the upper limit of S. We assumed the lower limit of integrated intensities to be $\frac{3}{4}$ of the full Lorentzian integration. The lower ends of the error bars include the errors in energy integration as well as statistical errors. Curves in the figure are drawn to guide the eye. In $Y(Mn_{0.9}Al_{0.1})_2$, S does not depend on temperature up to above 760 K within the experimental error whereas in YMn_2, S decreases by about 30% at T_N and then slowly increases with increasing temperature above T_N.

IV. DISCUSSION

A. Spin-glass transition

Spin-glass behavior of $Y(Mn_{1-x}Al_x)_2$ probed by static susceptibility and neutron-diffraction measurements has already been reported.[16] Therefore, we discuss here only the energy width Γ, of the scattered neutrons across the spin-glass transition temperature. As shown in Fig. 2, the temperature variation of Γ is unusually large compared with other spin glasses. In a usual spin glass, the change in Γ is too small to be detected by a conventional neutron spectrometer. For example, in a typical spin-glass alloy $Cu_{0.95}Mn_{0.05}$, the spin dynamics was studied by neutron spin echo techniques.[21] In this measurement, the existence of a very wide range of spin relaxation time has been observed. At $T_{\mathrm{SG}}=27$ K, the relaxation spectrum extends over several decades and about half the spectral component has relaxation times shorter than 10^{-9} sec (which corresponds to a characteristic energy of $E\sim\hbar/\tau\sim10^{-3}$ meV); the fraction decreases below T_{SG}. In the concentrated spin-glass alloy $Ni_{0.784}Mn_{0.216}$, which is ferromagnetic below 330 K, the ac susceptibility suggests the onset of a reentrant spin-glass phase at temperatures lower than 40 K. The temperature variation of the quasielastic scattering spectra was directly measured in this material using a high resolution triple axis spectrometer.[22] The temperature variation of a Lorentzian line width Γ could be expressed by

$$\Gamma=\Gamma_0\exp(-E_a/k_BT) \ , \tag{7}$$

with $\Gamma_0\simeq0.33$ meV and $E_a\simeq21.5$ meV, at least between 40 and 100 K. The energy width for $Y(Mn_{0.9}Al_{0.1})_2$ was found to follow the same formula in the temperature range $50\sim300$ K. Parameters determined from the fitting procedure are $\Gamma_0=49.0$ meV and $E_a=24.6$ meV. Here Γ_0 is more than 100 times larger than that of $Ni_{0.784}Mn_{0.216}$, whereas E_a is nearly the same. The curve in Fig. 2 represents the calculation from these parameters, which agrees fairly well with the observation for almost the entire temperature range. The theoretical form of the temperature dependence is based on the simple model that the freezing of spins takes place as a consequence of the existence of an energy barrier in the system. Γ_0 gives the measure of the energy difference of states separated by the energy barrier, E_a.

According to the model, an unusually large value of Γ_0 indicates that in $Y(Mn_{1-x}Al_x)_2$ the competition between positive and negative exchange interactions is extremely large compared with other spin glasses. This conjecture is also supported by the fact that the magnetic structure of YMn_2 is antiferromagnetic with a long period modulation where the competing interactions play an important role.

Needless to say, the above-mentioned model oversimplifies the real system and may be only one of several possible parameterizations of $\Gamma(T)$. However, we believe that the existence of anomalously large frustrations is one of the characteristics of the present $Y(Mn_{1-x}Al_x)_2$ system.

B. Spin fluctuations

In the present neutron scattering study, the most important characteristics of spin fluctuations, temperature variations of spatial correlation, and local amplitude, for YMn_2 and $Y(Mn_{0.9}Al_{0.1})_2$, have been clarified. Here we summarize our results and compare those with other ex-

perimental observations and also with the recent theory.

The spatial correlations of the spin fluctuations can be represented by the parameter κ_1, the inverse correlation length which we have shown in Fig. 4. In YMn_2, κ_1 is small and slightly increases with temperature above T_N. This observation means that in YMn_2 a considerable degree of spatial correlation between spin fluctuations persists up to far above T_N. In contrast, the spatial correlations in a local-moment Heisenberg magnet (as demonstrated by MnF_2) rapidly decreases as the temperature increases above T_N. In $Y(Mn_{0.9}Al_{0.1})_2$, which may be regarded as a local-moment system from previous macroscopic experimental results, the observed temperature variation behavior of κ_1 is much more similar to that of YMn_2 than to that of MnF_2.

The temperature variation of the local amplitude of spin fluctuations (spin S) for YMn_2 and for $Y(Mn_{0.9}Al_{0.1})_2$ is seen to be quite different from each other. In YMn_2, S decreases discontinuously at $T=T_N$ to ~ 0.8 from the low temperature value of 1.35, then increases gradually with temperature. On the other hand, in $Y(Mn_{0.9}Al_{0.1})_2$, S does not change within the experimental error in the temperature range 10–760 K.

As we mentioned in Sec. I, a neutron-scattering study of YMn_2 and $Y(Mn_{0.9}Al_{0.1})_2$ has also been reported by Deportes *et al.*[12,13] They used polarization analysis technique and a powder sample as we did in the present study. However, the experimental procedure and the data analysis are somewhat different from ours and the temperature range is limited to below 300 K. The energy integrated scattering intensity was collected utilizing a coarse energy resolution spectrometer ($2\Gamma_{res}=56$ meV) without analyzing the scattered neutron energy. After converting the intensity to absolute scale, they calculated the moment value from either the integration of $M(\mathbf{Q})$ in $\mathbf{Q}$ space or the integration of magnetization density [Fourier transformation of $M(\mathbf{Q})$] in real space. Since the energy spectrum of scattered neutrons is fairly well confined within the energy window as was confirmed by our experiment, this experimental method is assured to give the correct value for the moment. However, since their data analysis procedure does not resolve the scattering contributions from different magnetic zones, quantitative information for spin correlations could not be determined in this experiment. Moreover, because of the elimination of the energy analysis, information on dynamical properties of spin fluctuations cannot be obtained either. Spin for YMn_2 and $Y(Mn_{0.9}Al_{0.1})_2$ determined by Deportes *et al.* are also shown in Fig. 5, which agree with our result within experimental error.

A phenomenological theory of magneto-volume effects[23] suggests that thermal expansion measurements produce useful information on the variation of the local amplitude of spin fluctuations, or the local moment. In this theory the magnetic volume change is proportional to the square of the moment $\omega_m = km^2$. The value of magneto-volume coupling constant k is roughly $1\%/\mu_B$ for $3d$ transition metals. This method has been applied to several weakly itinerant ferromagnets such as $ZrZn_2$ (Ref. 24) and MnSi.[25] Shiga *et al.* applied this method to the present $Y(Mn_{1-x}Al_x)_2$ system and estimated the temperature variation of the local Mn moment.[10] In YMn_2, S drops to ~ 0.4 from the low-temperature value of 1.35 at $T=T_N$ and then gradually increases up to $S=1$ at 300 K. On the other hand, in $Y(Mn_{0.9}Al_{0.1})_2$, S does not change appreciably from the low-temperature value $S \simeq 1.4$ up to 300 K.

The result qualitatively agrees with what is found by neutron-scattering experiments. However, probably due to the choice of an improper value of the magneto-volume coupling constant, considerable difference appeared in the absolute value of S. We can see from these results that the thermal expansion method is very sensitive in detecting the presence of a change in the moment value. However, we must be aware of the difficulty in choosing the correct magneto-volume coupling constant for a particular material.

Although the property of spin fluctuations is fully described by the space-time correlation function of spin-density fluctuations, the important characteristics can be reduced to two variables, namely the local amplitude of spin fluctuations S (or local moment) and the spatial correlation of spin fluctuations (or short-range order). For most materials, these parameters can practically be obtained at currently available neutron facilities, while it is generally difficult to collect full information of the space-time correlation function due to the limitation of neutron energy and/or intensity.

Theoretically, an unambiguous calculation of these parameters has been performed for weakly itinerant electron magnets and for the local-moment case. For the intermediate case, the calculations have been made with adiabatic approximations for several materials introducing two phenomenological parameters, the longitudinal and transverse stiffness constants of the spin fluctuations.

For weakly-itinerant-electron magnets, S^2 increases almost linearly with temperature up to far above T_c, and the short-range order persists up to more than $\sim 10T_c$. On the other hand, for the local-moment case the local amplitude of spin fluctuation does not change with temperature and the spatial correlation exists only near the transition temperature.

Comparing our results with data from other magnetic materials, we can classify YMn_2 as a weakly itinerant electron magnet at $T > T_N$, as was suggested by macroscopic observations. We also claim that the first-order transition at $T \sim 100$ K is a transition of the electronic state from mainly localized to itinerant character. If the transition to the low-temperature phase is suppressed, the antiferromagnetic order might not be attained until $T_N^{\text{itinerant}} \ll T_N \sim 100$ K.

The temperature variation of S in $Y(Mn_{0.9}Al_{0.1})_2$ indicates that this material should be classified as a local-moment system. However, the temperature variation of short-range order suggests that the material is not a simple local-moment magnet. This apparent contradiction may, at least partly, stem from the presence of strong magnetic frustration in this system. However, as was demonstrated by the high-temperature neutron scattering study of Pd_2MnSn Heusler alloy,[4] the spin fluctuation behavior of metallic magnets, even if the materials are classified as "local-moment system," has been revealed to

be not identical to that of insulating Heisenberg magnets. Apparent similarity to the insulator magnets does only hold within a limited temperature and energy range. We stress that neutron-scattering experiments up to high temperature and high energy are crucial to the unified understanding of itinerant electron magnetism.

ACKNOWLEDGMENTS

We are grateful for stimulating discussions with Professor M. Shiga. One of the authors (K.M.) thanks the Neutron Scattering Group of Brookhaven National Laboratory for their hospitality during his stay. This work was supported by the U.S.–Japan Cooperative Neutron Scattering Program, and a Grant-in-Aid for Scientific Research from the Japanese Ministry of Education, Science, and Culture. Work at Brookhaven National laboratory was supported by the Division of Materials Sciences, U.S. Department of Energy under Contract No. DE-AC02-76CH00016.

[1]T. Moriya, J. Magn. Magn. Mater. **14**, 1 (1979).

[2]T. Moriya, *Spin Fluctuations in Itinerant Electron Magnetism* (Springer, Berlin, 1985).

[3]G. Shirane, Physica **137B**, 43 (1986).

[4]M. Kohgi, Y. Endoh, Y. Ishikawa, H. Yoshizawa, and G. Shirane, Phys. Rev. B **34**, 1762 (1986).

[5]Y. Ishikawa, Y. Noda, Y. J. Uemura, C. F. Majkrzak, and G. Shirane, Phys. Rev. B **31**, 5884 (1985).

[6]Y. Nakamura, M. Shiga, and S. Kawano, Physica **120B**, 212 (1983).

[7]Very recently, Ballou *et al.* have shown that YMn_2 orders antiferromagnetically with a very-long ($\sim$400 Å) period spiral structure: R. Ballou, J. Deportes, R. Lemaire, Y. Nakamura, and B. Ouladdiaf, J. Magn. Magn. Mater. **70**, 129 (1987).

[8]M. Shiga, H. Wada, and Y. Nakamura, J. Magn. Magn. Mater. **31-34**, 119 (1983).

[9]K. Yoshimura, M. Takigawa, H. Yasuoka, M. Shiga, and Y. Nakamura, J. Magn. Magn. Mater. **54-57**, 1075 (1986).

[10]M. Shiga, H. Wada, H. Nakamura, K. Yoshimura, and Y. Nakamura, J. Phys. F **17**, 1781 (1987).

[11]K. Yoshimura, M. Takigawa, H. Yasuoka, M. Shiga, and Y. Nakamura, private communication.

[12]J. Deportes, B. Ouladdiaf, and K. R. A. Ziebeck, J. Magn. Magn. Mater. **70**, 14 (1987).

[13]J. Deportes, B. Ouladdiaf, and K. R. A. Ziebeck, J. Phys. (Paris) **48**, 1029 (1987).

[14]K. Motoya, T. Freltoft, P. Böni, and G. Shirane, J. Phys. Soc. Jpn. **56**, 885 (1987).

[15]T. Freltoft, P. Böni, G. Shirane, and K. Motoya, Phys. Rev. B **37**, 3454 (1988).

[16]K. Motoya, J. Phys. Soc. Jpn., **55**, 3733 (1986).

[17]R. M. Moon, T. Riste, and W. C. Koehler, Phys. Rev. **181**, 920 (1969).

[18]J. P. Wicksted, P. Böni, and G. Shirane, Phys. Rev. B **30**, 3655 (1984).

[19]I. Halperin and P. C. Hohenberg, Phys. Rev. **177**, 952 (1969).

[20]P. Résibois and C. Piette, Phys. Rev. Lett. **24**, 514 (1970).

[21]F. Mezei and A. P. Murani, J. Magn. Magn. Mater. **14**, 489 (1984).

[22]B. Hennion, M. Hennion, F. Hippert, and A. P. Murani, J. Phys. F **14**, 489 (1984).

[23]M. Shiga, J. Phys. Soc. Jpn. **50**, 2573 (1981).

[24]S. Ogawa, Physica **119B**, 68 (1983).

[25]M. Matsunaga, Y. Ishikawa, and T. Nakajima, J. Phys. Soc. Jpn. **51**, 1153 (1982).